sensors

MDPI

Article

Microfluidic High-Q Circular Substrate-Integrated Waveguide (SIW) Cavity for Radio Frequency (RF) Chemical Liquid Sensing

Muhammad Usman Memon and Sungjoon Lim *

School of Electrical and Electronics Engineering, College of Engineering, Chung-Ang University, 84-Heukseok-ro, Dongjak-gu, Seoul 156-756, Korea; musmanm@outlook.com

* Correspondence: sungjoon@cau.ac.kr; Tel.: +82-2-820-5827

Received: 16 October 2017; Accepted: 4 January 2018; Published: 6 January 2018

Abstract: In this study, a high-Q circular substrate-integrated waveguide (SIW) cavity resonator is proposed as a non-contact and non-invasive radio frequency (RF) sensor for chemical sensing applications. The design of the structure utilizes SIW technology along with a circular shape to achieve a high unloaded Q factor, which is one of the important requirements for RF sensors. The resonant frequency of the proposed circular SIW cavity sensor changes when a liquid material or a chemical (microliters) is inserted in the sensitive area of the structure. The sensing of liquid materials with different permittivities is accomplished via the perturbation of the electric fields in the SIW configuration. When a microwell that is 4 mm in radius is installed vertically through the center of the bare circular SIW cavity, the operating frequency varies from 5.26 to 5.34 GHz. Similarly, when the microwell contains ethanol, the frequency shifts from 5.26 to 5.18 GHz, and the amplitude of reflection coefficient is shifted from −29 dB to −17 dB; when the microwell contains mixing deionized (DI)-water, the frequency moves from 5.26 to 4.98 GHz (which is also 0% Ethanol in our study), and the amplitude of reflection coefficient is shifted from −29 dB to −8 dB. A high unloaded Q factor is maintained throughout all experimental results. To demonstrate our idea, different concentrations of ethanol are tested and recorded. The experimental validation yields a close agreement between the simulations and the measurements.

Keywords: chemical sensor; SIW; circular cavity; RF sensor; wireless sensor; ethanol

1. Introduction

Chemical sensors have been used for many years to identify the purity ranks of numerous fluids to simplify the arrangement of those fluids for a wide range of industrial applications. It is necessary to store and classify these fluids or chemicals in accordance with the Globally Harmonized System of Classification and Labelling of Chemicals. The use of unidentified and unlabeled chemicals in experiments may have unforeseen consequences, and some of these chemicals may have severe effects on the human body. For example, methyl alcohol is toxic to the skin and body and can cause blindness, unconsciousness, and even death [1]. Consequently, fluidic chemical materials should be labeled so that they are recognized properly. Furthermore, a material safety manual should always be provided to the experimenters.

Traditional liquid chemical sensors for investigating bioassays or chemical assays and determining liquid quality require a large amount of fluid for filling the taps or tubes [2,3]. Therefore, during the process of analysis and measurement, a large amount of fluid is wasted. To solve this problem of wastage, microfluidic structures have been proposed. A silicon-microfabricated diffusion-based photosensitive chemical device was proposed for measuring chemical concentrations [4]. This optical sensing device can measure the analytical concentrations in a tiny volume of a compound taster.

Furthermore, a liquid-core optical ring-resonator device is discussed in [5]. A bonded silica tube acts as a ring resonator and transmits the fluid sample. The photosensitive characterization of the ring resonator is verified with a water–ethanol combination. This optically resonating device exploits the low liquid consumption, high sensitivity, and compact dimensions.

Figure 1 presents the substrate-integrated waveguide (SIW) configuration. An SIW is a favorable contender for improvements in planar radiofrequency (RF) circuits for wireless communication applications [6–12]. Figure 1 clearly shows that the SIW structure comprises two walls of metallic vias that connect the bottom and top conductors, and there is very low-loss dielectric material between the two conductors [13]. Because of the simple planar fabrication and its easy integration with other circuits, SIW modules are widely preferred for low-loss and high-quality reflections, in addition to a metallic waveguide and planar printed circuit board (PCB). Compared with microstrip structures and co-planar striplines, SIWs are easy to handle, low-cost, easy to fabricate, easily miniaturized, and low-profile. SIWs also provide the advantages of the traditional metallic waveguide structure, i.e., a high quality factor (QF), lowermost losses, appropriate shielding, and all-out power-handling capability. One of the most important features of these structures is that a full circuit can be constructed in a planar configuration, which is very important for integration with other circuits, antennas, transitions, and rectangular or circular waveguides having planar configurations obtained through typical PCB fabrication procedures.

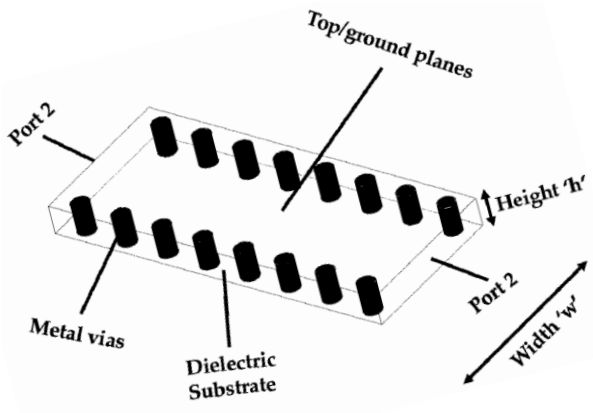

Figure 1. Illustration of the SIW structure.

SIW modules also permit multiple mount-in chipsets on a single board, which helps them to be merged with diverse circuit systems that have dissimilar principles and reduce the total loss. Recently, excellent studies have been reported in the scientific community regarding the miniaturization of SIW cavities [14]. This extensive investigation has forced the enhancement of design methods in SIW technology, and a new technique and procedure were presented recently to make SIWs reusable and more compact [15–18].

Polydimethylsiloxane (PDMS) microfluidic reservoirs make it possible to perform liquid testing experiments on the microliter or nanoliter scale in RF electronics. A shift in the resonant frequency may be observed by just testing a very small quantity of the fluid. PDMS, which is a commercial silicone elastomer with a low Young's modulus (<2 MPa), is a suitable candidate for making fluidic geometries [19]. PDMS exhibits a low surface energy and low modulus and is flexible. These properties allow it to be effortlessly attached onto electronic planes. It has a high loss tangent (0.0373) and a low dielectric constant (2.66) [20]. As previously mentioned, RF circuits permit the incorporation of fluidic reservoirs in order to sense different liquid materials, e.g., chemicals or bio-cells. An RF sensing device using E-shaped fluidic reservoir with a compact size and low loss was proposed in [21].

A very high-Q, non-invasive, and non-contact circular SIW cavity resonator is proposed for liquid chemical detection. The original configuration employs a circular waveguide combined with an SIW

construction, which offers various features: (1) lightness; (2) low radiation losses; and (3) a high QF, as previously discussed [13]. A circular SIW was chosen during the parametric analysis, because it produced a high unloaded Q factor of 1080, which the other configurations (square, rectangular, and triangular) failed to produce. The circular shape is derived from the circular waveguide resonator theory [22]. By combining the circular waveguide resonator with SIW technology, a very high unloaded Q factor of 1080 was realized in a planar configuration. In the presented research work, a PDMS microwell is installed in the center of the circularly constructed SIW to achieve a higher frequency-shifting ability while maintaining a high Q. A PDMS microwell can accommodate a maximum of 3 µL of liquid material. Therefore, the operating frequency of the proposed device is significantly affected by testing a very small quantity of fluid at the center of the circular SIW cavity. Quality control is one of the commercial application for our proposed sensor [23], but it can also be utilized in local chemistry laboratories for identification and labeling of liquid chemicals. Microwave cavity modules with such a configuration have been previously reported, along with frequency-tunable RF resonators [24–28].

2. Sensor Design

2.1. Circular SIW Cavity Resonator Design

The transverse magnetic (TM_{01}) and transverse electric (TE_{11}) modes are the dominant modes in a circular waveguide, as described in [29]. After deriving the Bessel's differential equation and Bessel functions, we express the lowest cutoff frequency of the two dominant modes TM_{01} and TE_{11} as follows:

$$(f_c)_{TM_{01}} = \frac{0.383}{a\sqrt{\mu\varepsilon}} \tag{1}$$

$$(f_c)_{TE_{11}} = \frac{0.293}{a\sqrt{\mu\varepsilon}} \tag{2}$$

where a is the radius of the circular waveguide, and μ and ε are the permeability and permittivity, respectively, of the dielectric material. Simultaneously, the resonant frequency of dominant $TM_{\mathrm{nm}\ell}$ and $TE_{\mathrm{nm}\ell}$ modes in the circular waveguide cavity are defined as [29]:

$$f_{nm\ell} = \frac{c}{2\pi\sqrt{\mu_r\varepsilon_r}}\sqrt{\left(\frac{P_{nm}}{a}\right)^2 + \left(\frac{\ell\pi}{d}\right)^2} \tag{3}$$

$$f_{nm\ell} = \frac{c}{2\pi\sqrt{\mu_r\varepsilon_r}}\sqrt{\left(\frac{P\prime_{nm}}{a}\right)^2 + \left(\frac{\ell\pi}{d}\right)^2} \tag{4}$$

where c is the speed of light, P_{nm} and P'_{nm} are the roots of Bessel's function $J_{\mathrm{n}}(x)$ and $J'_{\mathrm{n}}(x)$, a is the radius of the circular cavity, d is the depth, and μ_r and ε_r are the permeability and permittivity, respectively.

Our proposed structure is a combination of a circular waveguide and SIW technology. The reason for not choosing a typical rectangular SIW cavity structure is its lower Q factor compared to that of the circular SIW cavity. Therefore, to achieve our goals of attaining higher unloaded Q factor and better ethanol sensitivity with SIW technology compared to RF resonators, a circular waveguide cavity resonator is used along with the SIW technology; the structure becomes planar, and thus has a TE_{10} as the dominant mode of operation in our proposed research. The QF comparison between rectangular and circular SIW cavities is shown in Figure 2.

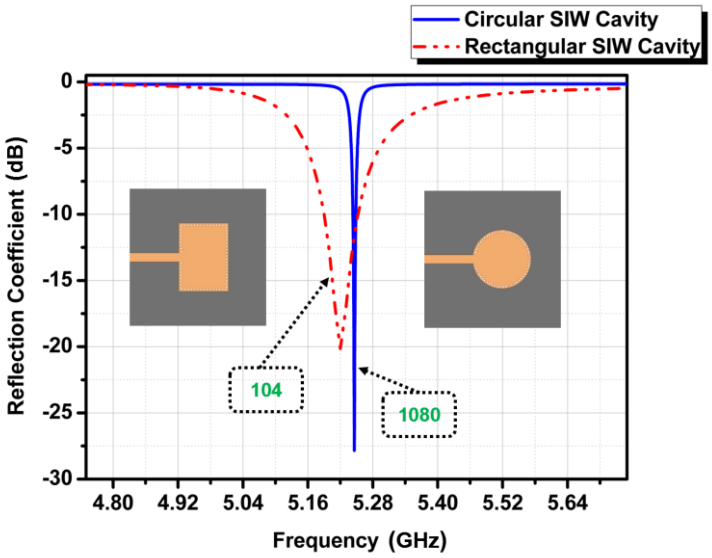

Figure 2. QF comparison between a rectangular SIW cavity and a circular SIW cavity at the same frequency.

The unloaded quality factor (Q) of a resonator can be defined as [29]:

$$Q = 2\pi f_0 \frac{W_m + W_e}{P_{loss}} \tag{5}$$

where f_0 is the resonant frequency and P_{loss} is the dissipated power. W_m and W_e are the average stored magnetic and electric energies, respectively. The Q factor can be calculated from the 3 dB bandwidth as:

$$Q = \frac{f_0}{f_{\mathrm{H,3dB}} - f_{\mathrm{L,3dB}}} \tag{6}$$

where $f_{\mathrm{H,3dB}}$ and $f_{\mathrm{L,3dB}}$ are the high and low frequencies at 3 dB below peak, respectively. In this work, we have used Equation (6) to calculate the unloaded Q factors for the simulated and measured reflection coefficient results. The above concept of unloaded Q-factor calculations for a one-port reflection resonator (our case) or for a two-port transmission and absorption cases is clearly explained in the these excellent works [30–33].

Figure 3 shows the design of the circular SIW cavity resonator. It is fed by a 50-Ω microstrip line. The Rogers RT/Duroid 5880 (Rogers Corporation, Connecticut, CT, USA) dielectric material (thickness = 1.575 mm, dielectric constant = 2.2, loss tangent = 0.0014) is selected to realize the idea. Initially, the structure was designed to resonate at 5 GHz. The detailed geometric parameters of the design are presented in Table 1. Figure 4 illustrates the electric-field (e-field) circulation of the simulated design when there is no microwell installed on the structure. Figure 4 clearly indicates that the magnitude of the e-field is concentrated at the center of the circular waveguide. A circular SIW cavity resonator is used in this study because of its lower scrounging loss, higher QF, and ease of PCB fabrication compared with other SIW shapes [14,17,34,35].

The operating frequency of the proposed device is directly proportional to the effective dielectric constant of the dielectric material. Furthermore, its effective permittivity is changed by testing fluidic chemicals or liquid biomaterials inside the microwell on the SIW cavity. Consequently, the suggested SIW cavity sensor can sense the permittivity of several fluidic chemicals by observing the change in the resonant frequency of the device. The e-fields of the structure are disturbed, which causes shifts in the frequency.

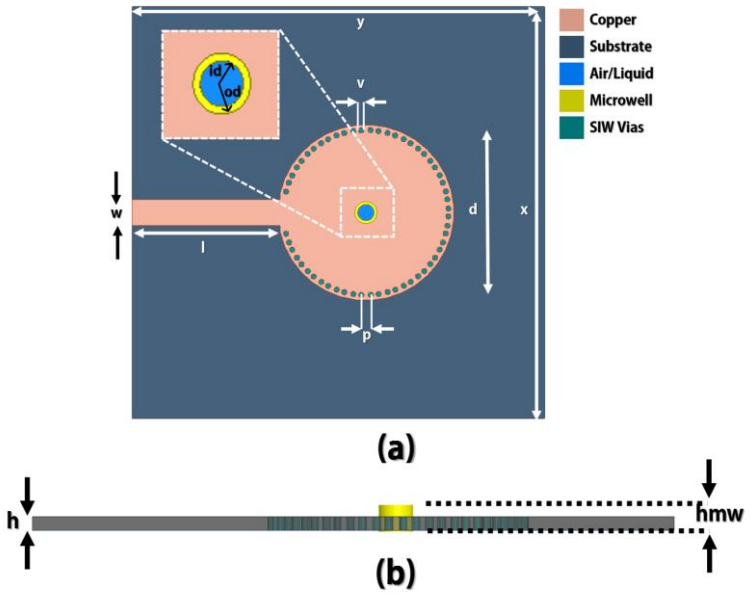

Figure 3. Design layout of the proposed sensor: (**a**) top view (zoomed microwell) and (**b**) cross-sectional view.

Table 1. Detailed geometric parameters of the design.

Number	Parameter	Dimension (mm)	Description
1	x	75	Width of substrate and metallic bottom ground
2	y	75	Height of substrate and metallic bottom ground
3	l	27	Length of microstrip line feeding
4	w	4.75	Width of microstrip line feeding
5	d	32	Diameter of circular SIW patch
6	p	1.7	Pitch (center to center) distance between vias
7	v	0.45	Diameter of SIW vias
8	id	2	Inner diameter of microwell
9	od	4	Outer diameter of microwell
10	h	1.575	Height of Rogers substrate
11	hmw	2.5	Height of microwell

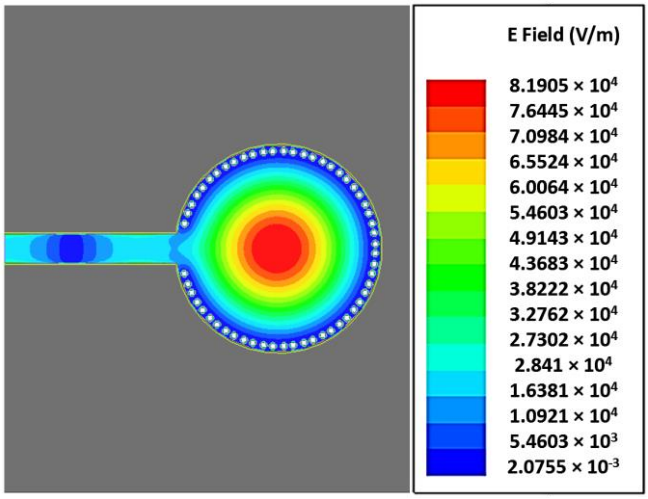

Figure 4. E-field distribution of the circular SIW resonator without microwell installed.

2.2. PDMS Microwell Design

A microwell with PDMS material is constructed and installed at a location where the magnitude of the e-field is strong (center). It is constructed to contain a maximum liquid volume of 3 µL. Each of the liquid samples tested in this study is 3 µL in volume. The microwell reservoir is 2 mm in height and 2 mm in diameter. As shown in Table 1, the diameter of the microwell is chosen to be 4 mm. This value is selected on the basis of parametric simulations, for checking the frequency sensitivity and maintaining a high Q, which are important features of an RF sensor. Figure 5 shows the detailed PDMS microwell construction for testing liquid materials.

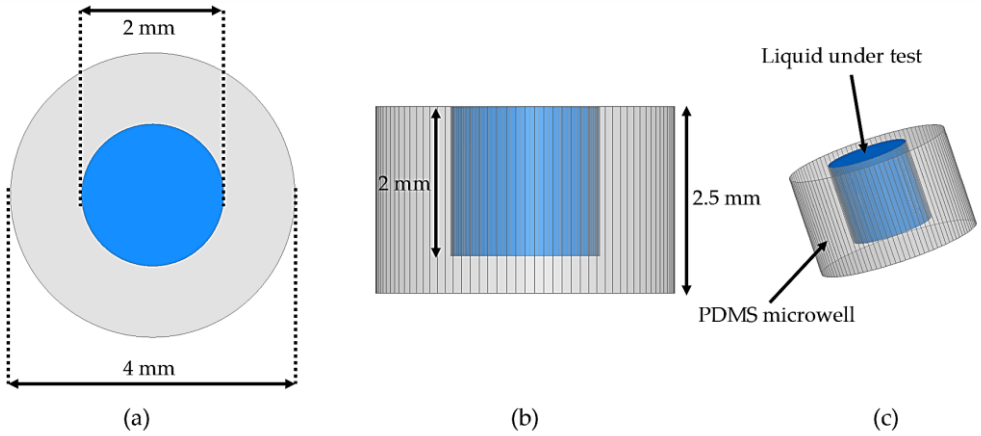

Figure 5. PDMS microwell: (**a**) top view, (**b**) cross-sectional view, and (**c**) bird's-eye view.

To justify the dimensions of the microwell, the microwell diameter is chosen as 4 mm on the basis of a parametric study. Figure 6 shows the simulation results for the case where the outer diameter of microwell varied from 2 to 6 mm. It must be noted that outer diameter is always a double of inner diameter. For instance, when the outer diameter is 2 mm, the inner diameter is 1mm; and when the outer diameter is 3 mm, the inner diameter is 1.5 mm, respectively. The parametric study revealed that 4 mm was the optimal outer diameter (2 mm inner diameter as seen in Figure 6) for installing the microwell in the structure to maintain a suitable QF of the circular SIW cavity and allow a significant frequency shift (between ethanol filled and empty microwell).

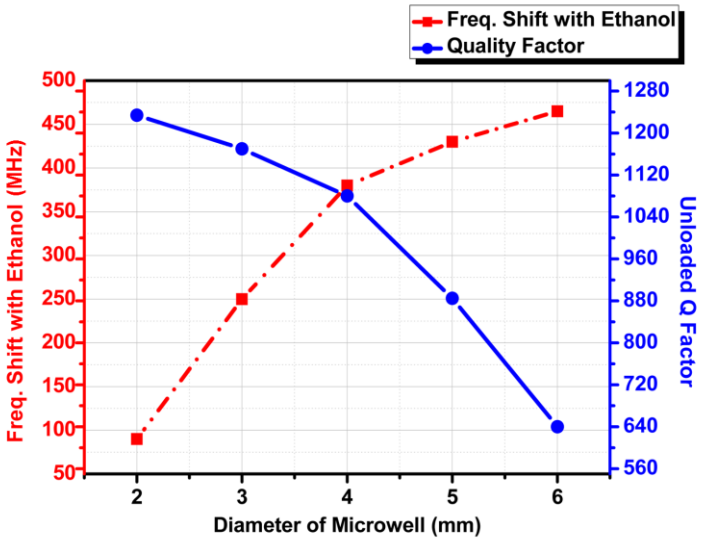

Figure 6. Simulated frequency shift and unloaded Q Factor at different diameters of the PDMS microwell.

3. Simulation Results

After the design process, a full wave computer simulation is performed using an ANSYS high-frequency structure simulator (HFSS). A microwell using a PDMS reservoir is examined, and its material specifications are extracted to produce a physical object in the computer software. Ethanol is also examined at a frequency of 5 GHz and is stored inside the microwell to validate our notion of sensing. The simulated reflection coefficients of the bare resonator (without the microwell), the ethanol-filled microwell, and the empty microwell are predicted to have distinct frequency responses.

Figure 7 shows the frequency responses for the three aforementioned cases, where the circular SIW resonator does not have a microwell, has a water-filled microwell, and has a microwell reservoir filled with ethanol. The corresponding operating frequencies observed are 5.24, 4.99, and 5.16 GHz. The unloaded QFs for these three cases are 1080 (bare), 431 (water-filled), and 463 (ethanol), respectively. The structure exhibits a very high Q, which is important for the ability of RF sensors to detect liquid materials having a high permittivity. Consequently, it can be predicted that this sensor device can function as a chemical concentration sensor and can sense many liquid materials with dissimilar relative permittivity.

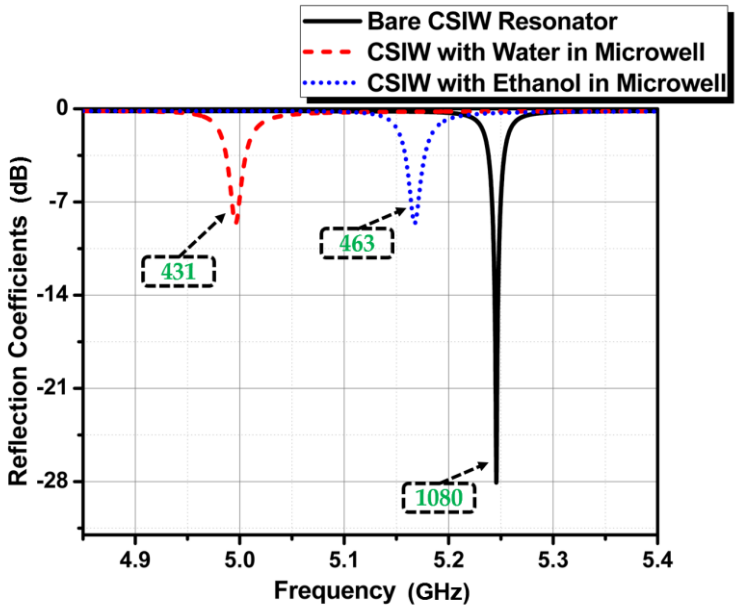

Figure 7. Simulated reflection coefficient for the bare circular SIW resonator, the water-filled microwell, and the microwell filled with ethanol. The unloaded Q factor is shown in a box for each result.

4. Experimental Demonstration

Figure 8 shows photographs of the proposed sensor. Figure 8a shows a fabricated circular SIW cavity resonator that has undergone a PCB etching process on a Rogers Duroid 5880 substrate. Figure 8b shows that a PDMS microwell has been inserted into the 4-mm hole at the center of the cavity. The drilled holes around the cavity are copper-plated metallic vias that connect the top copper patch with the bottom ground, making it an SIW cavity.

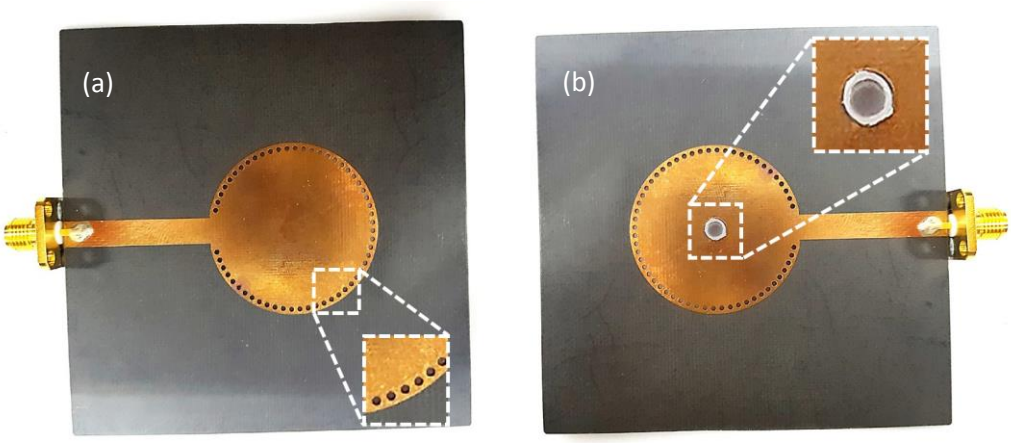

Figure 8. Fabricated sensor prototype: (**a**) circular SIW cavity resonator with metallic vias zoomed, and (**b**) with PDMS microwell in the center (microwell zoomed).

Ethanol is injected in the microwell, and the frequency responses for the previously discussed three cases are logged using an HP 8510C vector network analyzer (VNA) manufactured by Hewlett Packard, Palo Alto, CA, USA. In Figure 9, the simulation results are compared with the measurement results. The measured resonant frequencies exhibit good agreement with the simulated resonant frequencies. We can observe the difference between the simulated and measured reflection coefficients due to error in imaginary values of complex permittivity. In general, the real values of complex permittivity determines the resonant frequency, while the imaginary values of complex permittivity determines the reflection coefficient. However, it is difficult to extract the accurate imaginary values of complex permittivity rather than the real values of complex permittivity.

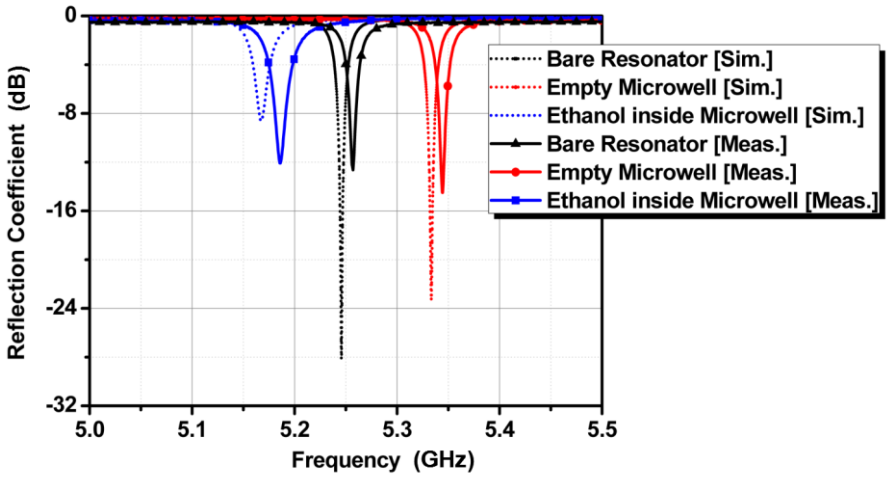

Figure 9. Measurement results plotted alongside simulated results.

Next, we aimed to employ this device as a purity sensor for ethanol. We prepared different concentrations of ethanol by mixing deionized (DI) water and measured the frequency responses. Figure 10 shows the measured reflection coefficients when the concentration of ethanol is sensed from 5% to 100%. The total amount of liquid that can fill the microwell is 3 µL, and 50% ethanol means 1.5 µL of ethanol mixed with 1.5 µL of DI water.

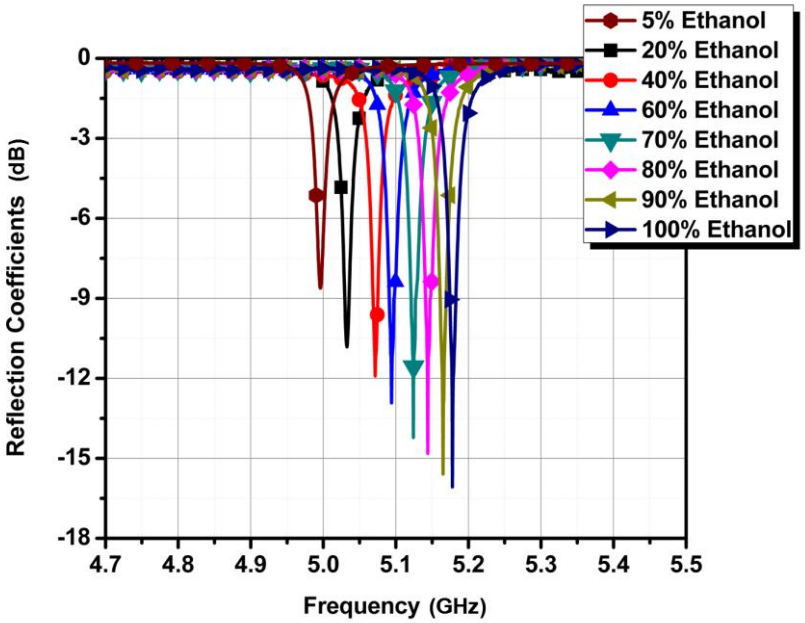

Figure 10. Measured reflection coefficients of different concentrations of ethanol, ranging from 5% to 100%.

The lowest bound of chemical recognition for the proposed sensor is 5% ethanol. To prepare 5% ethanol, 1 mL of DI water is stirred with 50 µL of pure ethyl alcohol. Absolute grade ethanol solvent (CH_3CH_2OH, part number 32,205) was purchased from Sigma–Aldrich (St. Louis, MO, USA). This solvent contained 789 g of solute in 1 L of water [36], which means that 5% ethanol corresponds to 39,450 ppm in our experimental demonstration. The material loss of 100% ethanol is higher than the material loss of 5% ethanol; however, because of the very high Q of the proposed SIW resonator, the QF is decent and does not degrade with different chemical concentrations. The relationship between the frequency and the ethanol concentration is almost linear, described as $y = 1.9 \times 10^{-3}\, x + 4.98$ for ethanol purities ranging from 5% to 100%. When the sensitivity of the proposed device as an ethanol sensor is resolute by the slope angle of the fitting curve, it is 1.9×10^{6} Hz/percentage. The sensitivity plot is shown in Figure 11 where error range is between −10 MHz to 10 MHz.

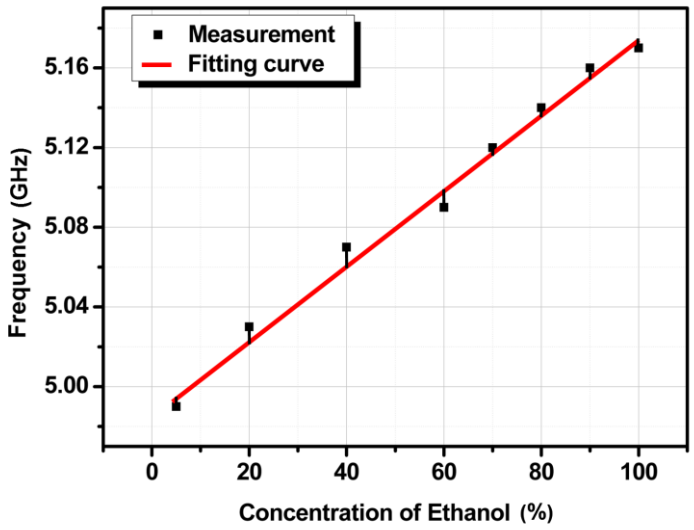

Figure 11. Frequency of the device with ethanol concentrations ranging from 5% to 100% with a fitting curve of $y = 1.9 \times 10^{-3}\, x + 4.98$.

To demonstrate the repeatability of the sensor, 10 experiments for 20% ethanol, 40% ethanol, and 80% ethanol are repeatedly performed under the same measurement setup. For the three aforementioned ethanol concentrations, the resonant frequency remained the same after emptying the microwell and re-injecting the solution in the microwell. The room temperature was controlled to 22 °C throughout our experiments. Figure 12 shows that the proposed sensor is reliable and the measurement results are reproducible using the same fabricated prototype.

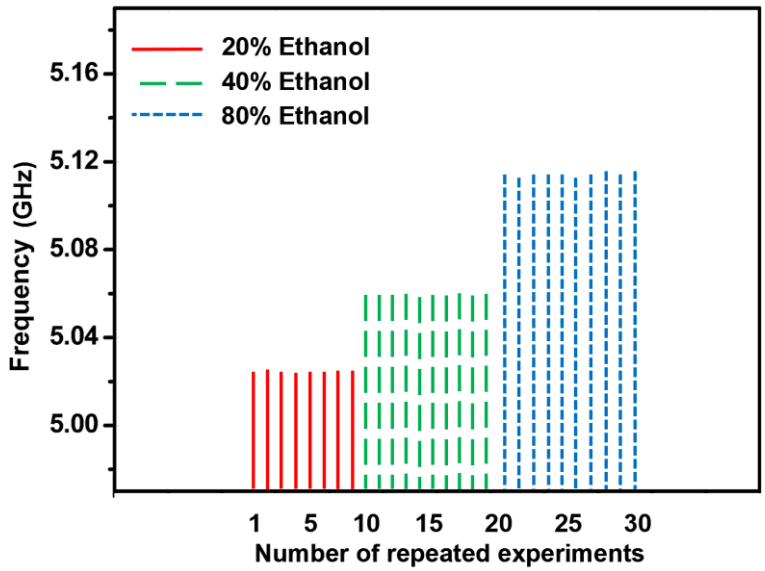

Figure 12. Repeatability test results of the fabricated sensor.

A comparison of proposed device with other recently reported SIW ethanol sensors is presented in Table 2. The unloaded Q factors are compared, when the resonators do not have an ethanol sample. All of the measurement results indicate that the proposed sensor device has a higher unloaded Q factor when there is no ethanol sample inside the resonator's sensitive area (bare resonator). Our proposed circular SIW cavity sensor also achieved a largest frequency shift and highest sensitivity for ethanol chemical. Some highly appreciated works using GHz-THz frequency band, sensing biomaterials, petrol, propanol, and other aqueous solutions using both optical and RF sensing mechanism are mentioned here [38–45].

Table 2. Performance of the proposed sensor compared with other SIW-based ethanol sensors.

Reference	Sensing	Frequency Shift (Δf) ‡ (MHz)	Sensitivity (MHz/ε_r)	Technology	QF	Volume (μL)
[21]	Ethanol liquid	145	26.36	SIW	39.12	10
[34]	Ethanol liquid	70	12.73	SIW	51	1
[37]	Ethanol liquid	38	5.84	SIW	334.6	500,000
This work	Ethanol purity	380	69.07	Circular SIW	1080	3

‡ Frequency shift (Δf) and sensitivity ($\Delta f / \Delta \varepsilon_r$) are calculated from air and ethanol; ε_r of air and ethanol are 1 and 6.5, respectively [38]. Unloaded QF are calculated when there is no ethanol sample (bare resonator).

5. Conclusions

A chemical and chemical-purity sensor is proposed. The device employs a circular SIW configuration. A microfluidic microwell made of PDMS is installed at the most subtle location of the SIW cavity (center). When a microfluid (maximum of 3 μL) is dropped on the PDMS microwell, the frequency of the device changes because of the change in the effective dielectric constant. The proposed sensor is constructed on a Rogers/Duroid 5880 dielectric material using the typical PCB

etching procedure, and the microwell is constructed over the PDMS material using a laser-etching engine, which is a simple and brief procedure. Our proposed idea is confirmed by close agreement between the simulation and measurement results. In addition, the measured results indicate a distinguishable frequency response when the ethanol purity is varied from 5% to 100% or when a different bio-cell is measured. The proposed sensor is planar, non-invasive, very high-Q, contracted, reusable, and non-contacting, and it accepts a very minute liquid sample for sensing. It is a low-cost device that can easily be manufactured through a typical PCB procedure. In this study, it was successfully demonstrated that the proposed circular SIW cavity sensor can detect chemicals and the purity level of ethanol. The repeatability and reliability of the presented sensor was confirmed by conducting more than 10 similar experiments. The proposed sensor discriminates various liquid chemicals having different dielectric constants. However, it is the limitation of RF sensors that they cannot differentiate between mixtures of chemicals or biomaterials having similar dielectric constants. Thus, we have proposed this device particularly as an ethanol concentration sensor. Quality control is one of the commercial applications for our proposed sensor, but it can also be utilized in local chemistry laboratories for identification and labeling of liquid chemicals. We are confident that in the future, we will produce this sensor on a flexible or inkjet-printed low-cost paper substrate for its use in wearable electronics or e-health because of increased advances.

Acknowledgments: This work was supported by the National Research Foundation of Korea (NRF) grant funded by the Korea government (MSIP) (No.2017R1A2B3003856).

Author Contributions: Muhammad Usman Memon conceived the idea. Muhammad Usman Memon designed and fabricated the prototype sample. Muhammad Usman Memon performed measurements and wrote the paper. Sungjoon Lim proofread and revised the manuscript.

Conflicts of Interest: The authors declare no conflict of interest.

References

1. Wen, G.; Wen, X.; Shuang, S.; Choi, M.M.F. Whole-cell biosensor for determination of methanol. *Sens. Actuators B Chem.* **2014**, *201*, 586–591. [CrossRef]
2. Mullett, W.M.; Levsen, K.; Lubda, D.; Pawliszyn, J. Bio-compatible in-tube solid-phase microextraction capillary for the direct extraction and high-performance liquid chromatographic determination of drugs in human serum. *J. Chromatogr. A* **2002**, *963*, 325–334. [CrossRef]
3. Dahlgren, R.; Van Nieuwenhuyse, E.; Litton, G. Transparency tube provides reliable water-quality measurements. *Calif. Agric.* **2004**, *58*, 149–153. [CrossRef]
4. Weigl, B.H.; Yager, P. Silicon-microfabricated diffusion-based optical chemical sensor. *Sens. Actuators B Chem.* **1997**, *39*, 452–457. [CrossRef]
5. White, I.M.; Oveys, H.; Fan, X. Liquid-core optical ring-resonator sensors. *Opt. Lett.* **2006**, *31*, 1319–1321. [CrossRef] [PubMed]
6. Shigeki, F. Waveguide line. Japan Patent 06-053, 1994.
7. Uchimura, H.; Takenoshita, T.; Fujii, M. Development of a "laminated waveguide". *IEEE Trans. Microw. Theory Tech.* **1998**, *46*, 2438–2443. [CrossRef]
8. Deslandes, D.; Wu, K. Single-substrate integration technique of planar circuits and waveguide filters. *IEEE Trans. Microw. Theory Tech.* **2003**, *51*, 593–596. [CrossRef]
9. Xu, F.; Wu, K. Guided-wave and leakage characteristics of substrate integrated waveguide. *IEEE Trans. Microw. Theory Tech.* **2005**, *53*, 66–73.
10. Deslandes, D.; Wu, K. Accurate modeling, wave mechanisms, and design considerations of a substrate integrated waveguide. *IEEE Trans. Microw. Theory Tech.* **2006**, *54*, 2516–2526. [CrossRef]
11. Wu, K. Towards system-on-substrate approach for future millimeter-wave and photonic wireless applications. In Proceedings of the 2006 Asia-Pacific Microwave Conference (APMC), Yokohama, Japan, 12–15 December 2006; pp. 1895–1900.
12. Li, Z.; Wu, K. 24-GHz Frequency-Modulation Continuous-Wave Radar Front-End System-on-Substrate. *IEEE Trans. Microw. Theory Tech.* **2008**, *56*, 278–285. [CrossRef]

13. Memon, M.U.; Lim, S. Review of reconfigurable substrate-integrated-waveguide antennas. *J. Electromagn. Waves Appl.* **2014**, *28*, 1815–1833. [CrossRef]
14. Memon, M.U.; Lim, S. Frequency-Tunable Compact Antenna Using Quarter-Mode Substrate Integrated Waveguide. *IEEE Antennas Wirel. Propag. Lett.* **2015**, *14*, 1606–1609. [CrossRef]
15. Memon, M.U.; Ling, K.; Seo, Y.; Lim, S. Frequency-switchable half-mode substrate-integrated waveguide antenna injecting eutectic gallium indium (EGaIn) liquid metal alloy. *J. Electromagn. Waves Appl.* **2015**, *29*, 2207–2215. [CrossRef]
16. Han, J.Y.; Yoon, S.S.; Lee, J.W. Miniaturization of SIW-Based Linearly Polarized Slot Antennas for Software-Defined Radar. *J. Electromagn. Eng. Sci.* **2016**, *16*, 248–253. [CrossRef]
17. Memon, M.U. Effects of Metallic Caps for Liquid Metal in Substrate Integrated Waveguide Antenna. In Proceedings of the 2015 IEEE Asia Pacific Microwave Conference (APMC), Nanjing, China, 6–9 December 2015; Volume 2, pp. 2–4.
18. Park, S.; Park, J. Dual-Band Gap-Filler Antenna Design with Phi-Shaped Slot. *J. Electromagn. Eng. Sci.* **2015**, *15*, 111–114.
19. McDonald, J.C.; Duffy, D.C.; Anderson, J.R.; Chiu, D.T.; Wu, H.; Schueller, O.J.; Whitesides, G.M. Fabrication of microfluidic systems in poly(dimethylsiloxane). *Electrophoresis* **2000**, *21*, 27–40. [CrossRef]
20. Lotters, J.C.; Olthuis, W.; Veltink, P.H.; Bergveld, P. The mechanical properties of the rubber elastic polymer polydimethylsiloxane for sensor applications. *J. Micromech.Microeng.* **1997**, *7*, 145–147. [CrossRef]
21. Memon, M.U.; Lim, S. Microwave Chemical Sensor Using Substrate-Integrated-Waveguide Cavity. *Sensors* **2016**, *16*, 1829. [CrossRef] [PubMed]
22. Benson, F.A.; Benson, T.M. Rectangular and circular waveguides and cavity resonators BT-Fields. In *Waves and Transmission Lines*; Springer: Dordrecht, The Netherlands, 1991; pp. 50–82.
23. Global Harmonised System of Classification and Labelling of Chemicals. Available online: https://www.comcare.gov.au/preventing/hazards/chemical_hazards/globally_harmonised_system_of_classification_and_labelling_of_chemicals_ghs (accessed on 27 November 2017).
24. Kiourti, A.; Sun, M.; He, X.; Volakis, J.L. Microwave Cavity with Controllable Temperature for In Vitro Hyperthermia Investigations. *J. Electromagn. Eng. Sci.* **2014**, *14*, 267–272. [CrossRef]
25. Hwang, S.-H.; Kang, C.G.; Lee, S.-M.; Lee, M.-Q. Reconfigurable Wireless Power Transfer System for Multiple Receivers. *J. Electromagn. Eng. Sci.* **2016**, *16*, 199–205. [CrossRef]
26. Wang, Y.; Yoon, K.-C.; Lee, J.C. A Frequency Tunable Double Band-Stop Resonator (BSR) with Voltage Control by Varactor Diodes. *J. Electromagn. Eng. Sci.* **2016**, *16*, 159–163. [CrossRef]
27. Ali, M.A.; Cheng, M.M.-C.; Chen, J.C.-M.; Wu, C.T.M. Microwave Gas Sensor based on Graphene-loaded Substrate Integrated Waveguide Cavity Resonator. In Proceedings of the 2016 IEEE MTT-S International Microwave Symposium (IMS), San Francisco, CA, USA, 22–27 May 2016; pp. 1–4.
28. Jones, T.R.; Zarifi, M.H.; Daneshmand, M. Miniaturized Quarter-Mode Substrate Integrated Cavity Resonators for Humidity Sensing. *IEEE Microw. Wirel. Compon. Lett.* **2017**, *27*, 612–614. [CrossRef]
29. Pozar, D. *Microwave Engineering*, 4th ed.; Addison Wesley: New York, NY, USA, 1990.
30. Khanna, A.P.S.; Garault, Y. Determination of Loaded, Unloaded, and External Quality Factors of a Dielectric Resonator Coupled to a Microstrip Line. *IEEE Trans. Microw. Theory Tech.* **1983**, *31*, 261–264. [CrossRef]
31. Chua, L.H.; Mirshekar-Syahkal, D. Accurate and direct characterization of high-q microwave resonators using one-port measurement. *IEEE Trans. Microw. Theory Tech.* **2003**, *51*, 978–985. [CrossRef]
32. Sun, E.; Chao, S. Unloaded Q measurement-the critical points method. *IEEE Trans. Microw. Theory Tech.* **1995**, *43*, 1983–1986.
33. Bray, J.R.; Roy, L. Measuring the unloaded, loaded, and external quality factors of one- and two-port resonators using scattering-parameter magnitudes at fractional power levels. *IEE Proc. Microw. Antennas Propag.* **2004**, *151*, 345–350. [CrossRef]
34. Seo, Y.; Memon, M.U.; Lim, S. Microfluidic Eighth-Mode Substrate-Integrated-Waveguide Antenna for Compact Ethanol Chemical Sensor Application. *IEEE Trans. Antennas Propag.* **2016**, *64*, 3218–3222. [CrossRef]
35. Jiang, L.; Pau, S. Integrated waveguide with a microfluidic channel in spiral geometry for spectroscopic applications. *Appl. Phys. Lett.* **2007**, *90*, 8–11. [CrossRef]
36. Ethanol Product Information. Available online: http://www.sigmaaldrich.com/catalog/product/sial/32205?lang=ko&region=KR (accessed on 11 April 2016).

37. Liu, C.; Tong, F. An SIW Resonator Sensor for Liquid Permittivity Measurements at C Band. *IEEE Microw. Wirel. Compon. Lett.* **2015**, *25*, 751–753.
38. Salim, A.; Lim, S. Complementary split-ring resonator-loaded microfluidic ethanol chemical sensor. *Sensors* **2016**, *16*, 1802. [CrossRef] [PubMed]
39. Cui, Y.; He, Y.; Wang, P. A Quadrature-Based Tunable Radio-Frequency Sensor for the Detection and Analysis of Aqueous Solutions. *IEEE Microw. Wirel. Compon. Lett.* **2014**, *24*, 490–492. [CrossRef] [PubMed]
40. Klein, N.; Watts, C.; Hanham, S.M.; Otter, W.J.; Ahmad, M.M.; Lucyszyn, S. Microwave-to-terahertz dielectric resonators for liquid sensing in microfluidic systems. In Proceedings of the 2016 Conference on Terahertz Emitters, Receivers, and Applications VII, San Diego, CA, USA, 28–31 August 2016; Volume 9934.
41. Liu, W.N. A Novel Technology for Measurements of Dielectric Properties of Extremely Small Volumes of Liquids. *Int. J. Antennas Propag.* **2016**, *2016*, 1436798. [CrossRef]
42. Matvejev, V.; Zhang, Y.; Stiens, J. High performance integrated terahertz sensor for detection of biomolecular processes in solution. *IET Microw. Antennas Propag.* **2014**, *8*, 394–400. [CrossRef]
43. Mendis, R.; Astley, V.; Liu, J.; Mittleman, D.M. Terahertz microfluidic sensor based on a parallel-plate waveguide resonant cavity. *Appl. Phys. Lett.* **2009**, *95*, 1–4. [CrossRef]
44. Neshat, M.; Chen, H.; Gigoyan, S.; Saeedkia, D.; Safavi-Naeini, S. Whispering-gallery-mode resonance sensor for dielectric sensing of drug tablets. *Meas. Sci. Technol.* **2009**, *21*, 15202. [CrossRef]
45. Rawat, V.; Dhobale, S.; Kale, S.N. Ultra-fast selective sensing of ethanol and petrol using microwave-range metamaterial complementary split-ring resonators. *J. Appl. Phys.* **2014**, *116*, 1–6. [CrossRef]